Comparative analysis of microstructural segmentation techniques on SEM and optical micrographs

Katika Harikrishna*

Department of Metallurgical and Materials Engineering, Indian Institute of Technology Madras, Chennai, 600036, Tamil Nadu, India

Abstract. Since grain morphology, distribution, and interfaces have significant effects on mechanical and functional properties, accurate microstructural characterization is still indispensable to materials research. The segmentation of Al+SiC nanocomposites using backscattered electron SEM images and the segmentation of Al-Zn-Mg powder metallurgy alloys using optical micrographs are compared in this paper. This comparison, rather than reporting material-specific results, attempts to present a broader methodological perspective by trying to distill general insights into how various imaging modalities drive algorithmic choices. These accuracy aspects are not revisited here because both have already shown high accuracy in automated segmentation and grain boundary detection. Rather, focus is on how image modality, preprocessing specifications, segmentation pipelines, and post-processing techniques interact to determine the robustness, flexibility, and possible transferability of automated microstructural analysis workflows.

1 Introduction

Since grain morphology, distribution, and interfaces directly impact mechanical and functional properties, accurate microstructural characterization is still essential to materials research [1]. Automated microstructure segmentation is now feasible thanks to recent developments in computer vision and image processing, which reduces the need for time-consuming manual techniques. However, the imaging modality used determines how successful these automated techniques are; optical and scanning electron microscopy (SEM) pose different difficulties. Particle-matrix interface ambiguity and detector noise are two drawbacks of SEM, even though it offers compositional contrast with a high spatial resolution, especially when using the BSE mode. In fact, optical micrographs are characterized by uneven illumination, inconsistent etching, and varying grain contrast.

Several techniques have been developed for image segmentation—the process of dividing an image into regions with similar properties. Common segmentation approaches include region-based methods [2], thresholding [3], graph-theoretic techniques [4], edge detection [5], and energy-based models [6]. Threshold-based segmentation, in particular, classifies

* Corresponding author: kharikrishna@student.nitw.ac.in

image pixels into distinct groups according to predefined or computed intensity thresholds. This category includes methods such as histogram-based thresholding [7], iterative threshold selection [8], inter-class variance thresholding [9], and adaptive (dynamic) thresholding [10].

Two recent studies tackled these issues in different settings: one created a novel computer vision algorithm for optical images of hot-deformed Al–Zn–Mg alloys [11], while the other used sophisticated image processing to segment BSE micrographs of Al+SiC nanocomposites [12]. Very few studies have examined the significance of methodological comparison to date. This paper does not reevaluate accuracy, despite the fact that both achieved high accuracy in automated grain size determination. Rather, it emphasizes how various preprocessing filters, segmentation techniques, and post-processing refinements were selected according to the imaging modality through a comparative analysis of the underlying methodologies. The machine learning framework can use these processed images as ground truth [1].

2 Methodological framework

2.1 SEM image segmentation

The segmentation of Al + SiC nanocomposites was carried out on BSE micrographs, which inherently provide compositional contrast between the aluminum matrix and the SiC reinforcements. To prepare the images for analysis, the RGB data format of the acquired BSE images was first converted to grayscale (Figure 1b) to remove redundant channels. Preprocessing involved Gaussian filtering (Figure 1c) to suppress random noise and median filtering to reduce salt-and-pepper artifacts, thereby improving the clarity of the particle–matrix interfaces without distorting the true boundaries. Contrast enhancement techniques, particularly histogram equalization (Figure 1d), were applied to sharpen intensity differences between adjacent phases.

Global thresholding has been used for segmentation, separating the darker SiC particles from the lighter aluminum matrix. Adaptive thresholding was not necessary because the inherent compositional contrast in the BSE image already generates explicit phase boundaries [13]. Edge detection operators, most especially the Sobel filter, have been applied to accurately grain boundary trace with enhanced delineation of particle edges. Thereafter, morphological operations such as dilation and erosion have been used to close discontinuities in identified boundaries and remove noise-induced artifacts, respectively (Figure 1f & g). Finally, a post-processing step has been added to refine the results of segmentation. Small, isolated objects generated by noise or incomplete detection were removed using size-based filtering (Figure 1h), while boundary continuity has been restored by morphological closing. The combination of preprocessing steps, filtering, thresholding, and morphological refinement has offered robust segmentation of the BSE micrographs.

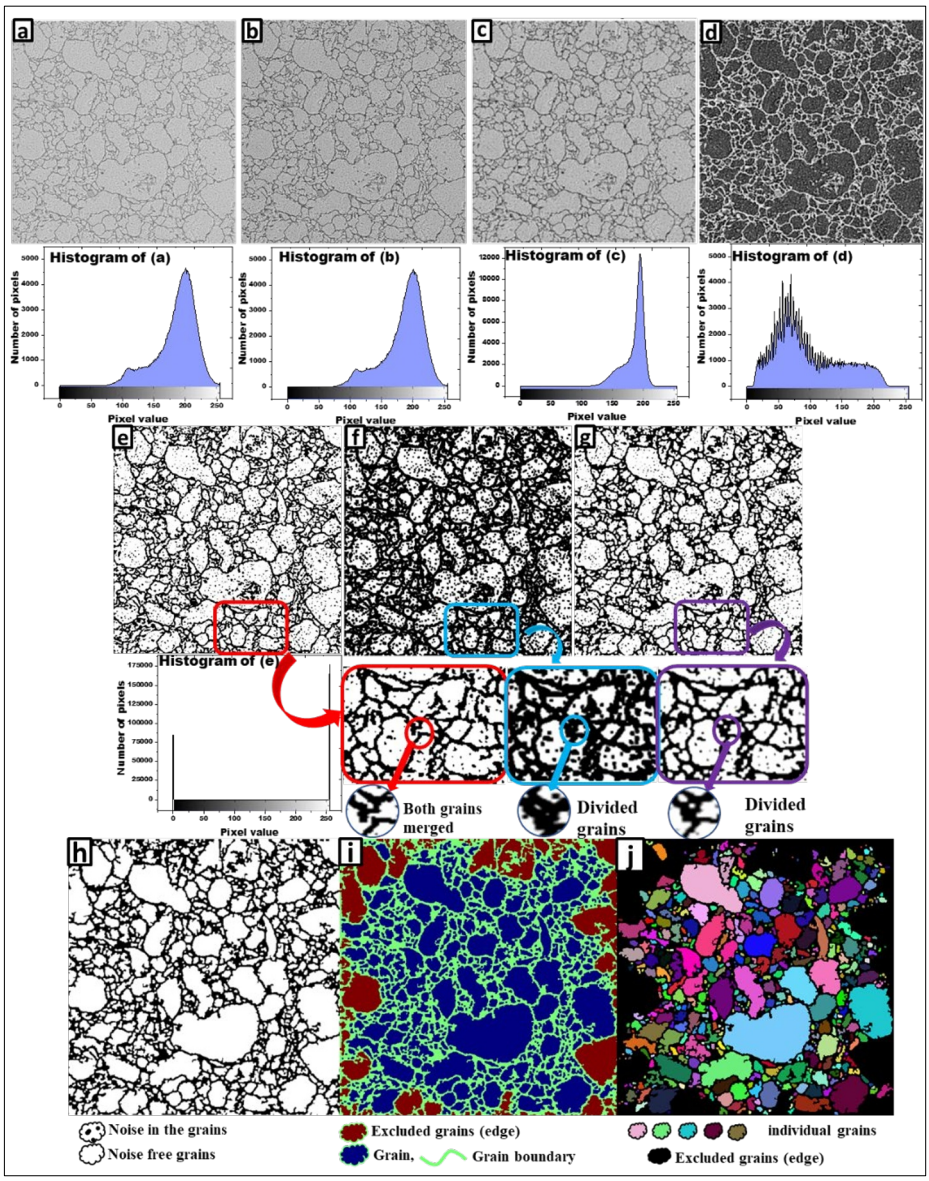

Fig. 1. Segmentation workflow for BSE micrographs: (a) Original, (b) Grayscale, (c) Noise filtering, (d) Contrast enhancement, (e) Thresholding, (f–g) Morphological refinement, (h) Otsu's thresholding, (i) Final segmented image, and (j) Distance transform analysis. [12].

2.2 Optical image segmentation (Al–Zn–Mg powder metallurgy alloys)

Optical micrographs of the Al-Zn-Mg alloy were segmented using an image-processing pipeline tailored for light microscopy data. Although both optical and BSE images represent microstructural features, optical images often exhibit lower inherent contrast; hence, slight preprocessing differences are used. First, the RGB-format optical images were converted to grayscale (Figure 2b) to remove redundant channels and prepare them for analysis. Median

blur filtering was then applied (Figure 2c) to suppress noise and smooth intensity variations, which enhanced the visibility of particle boundaries without changing their actual geometry.

Segmentation was then done by Otsu's thresholding. It automatically calculates the optimum threshold to separate grain and boundaries (Figure 2d). Since optical micrographs mostly show subtle variations in contrast, this was an effective preprocessing step. After thresholding, morphological operations were done to remove the isolated noise and for the continuity of grain boundaries (Figure 2e & f). Other refinements included binary filling, in order to rectify the voids within the particle area, flood-fill operation to suppress background artifacts (Figure 2g), and finally the distance transform analysis was done (Figure 2i) to retain fidelity in particle shapes and thereby avoid their over-segmentation. Thus, a step-by-step approach-median smoothing, Otsu thresholding, morphological refinement, and geometric correction managed to correctly segment the optical images that have less sharp phase boundaries compared to the SEM micrographs.

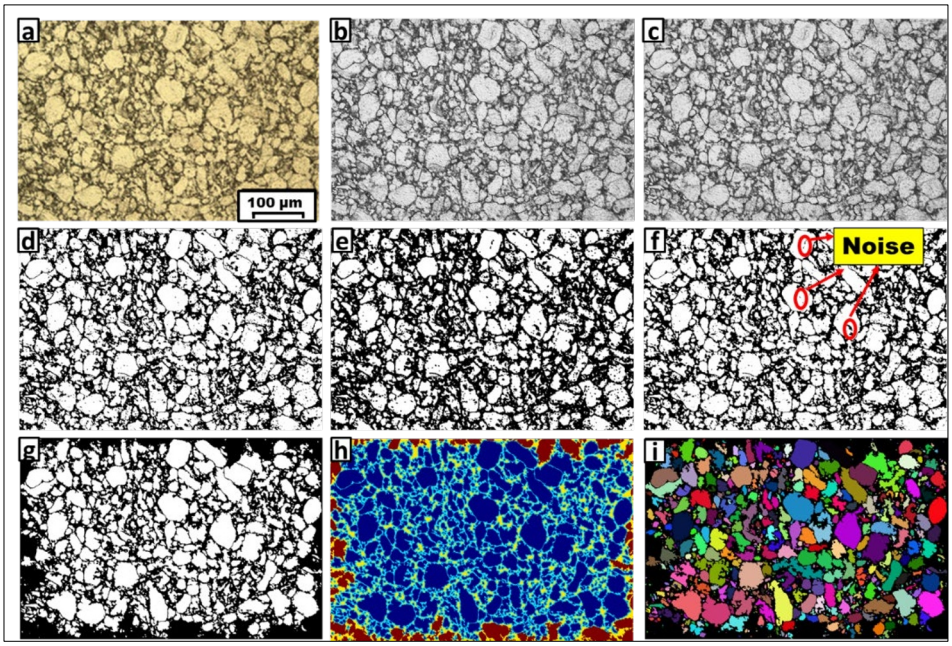

Fig. 2. Stepwise image-processing pipeline for segmenting optical micrographs of Al–Zn–Mg alloy: (a) Original RGB image, (b) Grayscale conversion, (c) Median blur filtering, (d) Otsu's thresholding, (e–f) Morphological refinement to remove noise and ensure boundary continuity, (g) Binary filling and background correction, (h) Segmented image, and (i) Distance transform analysis [11].

3 Comparative analysis & limitations and future work

A comparison of the SEM and optical image segmentation workflows from the present work indicates distinct methodological preferences, largely dictated by the intrinsic image characteristics of each modality. SEM BSE micrographs inherently bear high compositional contrast between phases, thus allowing for effective segmentation by employing comparatively simpler approaches, such as global thresholding with limited edge enhancement. Noise suppression and boundary fidelity are therefore the main emphases during SEM processing, making Gaussian filters along with CLAHE filters, when combined with global thresholding and Sobel edge detection, particularly effective. In contrast, optical micrographs often have lower, more variable contrast, dependent upon etching and

illumination quality, for example, thereby making adaptive thresholding strategies necessary to compensate for variability in brightness. These types of edge detection methods, such as Canny, are much more important in optical imaging to detect faint and/or discontinuous grain boundaries. Also, morphological refinement as a method of correcting illumination and polishing artefacts is more heavily used. Hence, while segmentation of SEM images relies on the inherent material contrast and requires fewer corrective steps, optical image segmentation places higher demands on an elaborate preprocessing and segmentation pipeline as a requirement for grain boundary detection. Finally, morphological refinement and size-based filtering emerge as an essential last step common to both methods by which reliable measurement of grain size is achieved; however, their emphasis and processing intensity differ radically depending on the modality of the image being processed. Table 1 presents in summary the comparative difference arising between SEM and optical image segmentation.

Table 1. Summarizing methodological différences.

Aspect	**SEM (BSE) Image Segmentation – Al + SiC Nanocomposites**	**Optical Image Segmentation – Al–Zn–Mg Alloys**
Imaging Modality & Nature	Backscattered Electron (BSE) mode SEM provides compositional contrast between Al matrix and SiC particles; high spatial resolution.	Optical microscopy produces illumination- and etching-dependent contrast; affected by surface quality and polishing.
Preprocessing Filters	Gaussian filter to reduce random noise; median filter for salt-and-pepper noise suppression.	Median blur filter for smoothing intensity variations; bilateral/median filtering for illumination normalization.
Algorithmic Complexity	Relatively simpler workflow; high contrast reduces need for adaptive methods.	More complex pipeline; requires adaptive and multi-step corrections.
Limitations	Sensitive to detector noise; only effective for BSE contrast-rich systems.	Sensitive to etching, illumination, and surface quality; may require calibration for different alloys.
Overall Insight	Effective for high-contrast, composition-sensitive imaging; robust with minimal correction.	Effective for low-contrast, illumination-sensitive imaging; requires adaptive segmentation and correction steps.

a) Limitations

Although the comparative methodology successfully highlights modality-driven differences, its applicability to other materials or imaging conditions may require additional calibration. The current study is restricted to two-dimensional image analyses on aluminum-based systems. In particular, optical images are still susceptible to surface artifacts, etching irregularities, and variations in illumination, which can cause segmentation errors even after preprocessing adjustments. Furthermore, neither workflow incorporates data-driven learning and instead relies on traditional image processing methods, which limits their ability to adapt to new datasets.

b) Future work

Future research will attempt to extend this comparative framework toward 3D microstructural reconstruction from FIB-SEM or X-ray tomography data in order to allow for a more complete assessment of grain topology. Naturally, boundary detection, feature recognition, and material generalization will benefit substantially from the integration of deep learning architectures such as U-Net, Mask R-CNN, or Vision Transformers. Another promising direction is the integration of multimodal data fusion, where optical, SEM, and EBSD data are combined; this may lead to the development of robust, fully automated microstructural segmentation pipelines that can be adapted easily to different imaging environments.

4 Conclusion

This paper compared two previously established methodologies for grain segmentation, one based on BSE images of Al–SiC nanocomposites and the other on optical micrographs of Al–Zn–Mg alloys. More specifically, the aim was to distill modality-specific insights in terms of preprocessing, filtering, and segmentation strategies rather than material-specific results.

1. Image modality is the main determinant of preprocessing needs: While BSE images require denoising and contrast stabilization, for optical images, illumination correction and color normalization play a more important role.
2. Filter effectiveness is modality-specific: median and Gaussian filters perform better on SEM/BSE images, while for optical images, bilateral filtering and adaptive histogram equalization are more effective.
3. The segmentation strategies vary, and it was found that adaptive thresholding and morphology worked well for SEM images, while edge-detection and watershed methods worked better for optical images.
4. Overall, both methodologies achieve reliable segmentation, but their workflows are not interchangeable; algorithmic choices must be carefully aligned with the imaging modality.

References

1. A. Shah et al., “Automated image segmentation of scanning electron microscopy images of graphene using U-Net Neural Network,” Mater. Today Commun., vol. 35, no. April, p. 106127, 2023, doi: 10.1016/j.mtcomm.2023.106127.
2. H. G. Kaganami and Z. Beiji, “Region-based segmentation versus edge detection,” IIH-MSP 2009 - 2009 5th Int. Conf. Intell. Inf. Hiding Multimed. Signal Process., pp. 1217–1221, 2009, doi: 10.1109/IIH-MSP.2009.13.
3. K. Bhargavi and S. Jyothi, “A Survey on Threshold Based Segmentation Technique in Image Processing,” Int. J. Innov. Res. Dev., vol. 3, no. 12, pp. 234–239, 2014, [Online]. Available: https://www.researchgate.net/publication/309209325.
4. V. R. Parihar and N. V Thakur, “Graph Theory Based Approach For Image Segmentation Using Wavelet Transform,” Int. J. Image Process., vol. 8, no. 5, pp. 255–277, 2014, [Online]. Available: http://www.cscjournals.org/manuscript/Journals/IJIP/Volume8/Issue5/IJIP-904.pdf.
5. Y. C. Huang, Y. S. Tung, J. C. Chen, S. W. Wang, and J. L. Wu, “An adaptive edge detection based colorization algorithm and its applications,” Proc. 13th ACM Int. Conf. Multimedia, MM 2005, pp. 351–354, 2005, doi: 10.1145/1101149.1101223.

6. X. Bresson, P. Vandergheynst, and J. P. Thiran, “A priori information in image segmentation: Energy functional based on shape statistical model and image information,” IEEE Int. Conf. Image Process., vol. 3, pp. 425–428, 2003, doi: 10.1109/icip.2003.1247272.
7. O. J. Tobias and R. Seara, “Image segmentation by histogram thresholding,” IEEE Trans. Image Process., vol. 11, no. 12, pp. 1457–1465, 2002, doi: 10.1109/TIP.2002.806231.
8. M. Rezaiee-Pajand, A. Entezami, and H. Shariatmadar, “An iterative order determination method for time-series modeling in structural health monitoring,” Adv. Struct. Eng., vol. 21, no. 2, pp. 300–314, 2018, doi: 10.1177/1369433217717118.
9. A. Z. Arifin and A. Asano, “Image segmentation by histogram thresholding using hierarchical cluster analysis,” Pattern Recognit. Lett., vol. 27, no. 13, pp. 1515–1521, 2006, doi: 10.1016/j.patrec.2006.02.022.
10. P. Yogarajah, J. Condell, K. Curran, A. Cheddad, and P. McKevitt, “A dynamic threshold approach for skin segmentation in color images,” Proc. - Int. Conf. Image Process. ICIP, pp. 2225–2228, 2010, doi: 10.1109/ICIP.2010.5652798.
11. K. Harikrishna, M. Joseph Davidson, G. Dhanush Reddy, and K. Veera Venkata Nagaraju, “Overcoming optical image challenges in automatic grain size measurement using a novel computer vision algorithm applied to hot deformation of Al-Zn-Mg Powder metallurgy alloy,” Mater. Lett., vol. 357, no. November 2023, p. 135743, 2024, doi: 10.1016/j.matlet.2023.135743.
12. K. Harikrishna, A. Nithin, and M. J. Davidson, “Automated microstructural segmentation and grain size measurement of Al + SiC nanocomposites using advanced image processing techniques on backscattered electron images,” Mater. Charact., vol. 222, no. February, p. 114845, 2025, doi: 10.1016/j.matchar.2025.114845.
13. H. F. Ng, “Automatic thresholding for defect detection,” Pattern Recognit. Lett., vol. 27, no. 14, pp. 1644–1649, 2006, doi: 10.1016/j.patrec.2006.03.009.